Euro. Jnl of Applied Mathematics (2000), *vol.* 11, *pp.* 529–559. Printed in the United Kingdom

Self-similar flows of multi-phase immiscible fluids

A. OZTEKIN[1], B. R. SEYMOUR[2] and E. VARLEY[1]

[1] *Department of Mechanical Engineering, Lehigh University, Bethlehem, PA 18017, USA*
[2] *Department of Mathematics, University of British Columbia, Vancouver, V6T 1Z2, Canada*

(*Received 16 February 2000; revised 13 July 2000*)

Exact analytical representations are obtained describing self-similar unsteady flows of multi-phase immiscible fluids in the vicinity of non-circular, but constant strength, fronts. It is assumed that Darcy's law holds for each phase and that the mobilities are known functions of the saturations. Equivalent representations are obtained for Hele-Shaw cell flows that are produced when a viscous fluid is injected into a region containing some other viscous fluid. The fluids may be Newtonian fluids or non-Newtonian fluids for which the coefficients of viscosity depend on the shear stress. Even though the flows are unsteady and two dimensional, the representations are obtained by using hodograph techniques.

1 Introduction

This paper describes flows in a porous medium that are produced when a stationary fluid composed of several immiscible phases is displaced by injecting other immiscible fluids into a region that is small compared with that occupied by the resident fluid. The analysis is based on a model of the 'secondary recovery' process that is used in the petroleum industry to drive oil towards a recovery well by injecting either water or gas, or a combination of both. A comprehensive review of the various mathematical models that are used to describe this process is given in the book by Barenblatt, Entov & Ryzhik (1990). More recent accounts are described in two special issues (1995, 1999) of the *European Journal of Applied Mathematics*. In the simplest Muskat–Leverett model, the governing equations form a system of coupled first order partial differential equations in space and time of convective-diffusive type for the variations in the saturations and partial pressures. These result from applying Darcy's law and the law of conservation of mass to each phase, and stipulating equations of state for the mobilities and capillary pressures in terms of the saturations. When the fluid contains just two phases and the flow is one-dimensional, the bulk velocity of the fluid depends only on time. Then, a nonlinear second order equation can be obtained that governs the variation in the saturation of one of the phases in time and distance. When the effect of capillary pressure is small, as is the case for the flows described in this paper, fronts develop across which the saturation varies rapidly. When the effect of capillary pressure is neglected completely, this equation reduces to the Buckley–Leverett simple wave equation and the fronts are propagating surfaces across which the saturation is discontinuous. In this limit, one dimensional flows can be analyzed by procedures that are standard in the study of gasdynamics.

When the flows are unsteady and not unidirectional, only in the limiting case when the total mobility is constant and capillary effects can be neglected are there any known exact analytical solutions to the governing equations. Usually, solutions are sought by using numerical procedures. However, because of the nature of the governing equations and the existence of fronts whose locations must be determined as part of the solution, these procedures remain unreliable (see Chavent and Jaffre, 1986): changing the grid orientation can produce completely different numerical outputs. This study uses hodograph techniques developed by Sidorov (1963) and Cumberbatch & Varley (1966) in their research on self-similar, two-dimensional, unsteady flows of a gas to construct exact solutions to the governing equations in the limit when the effect of capillary pressures can be neglected. These exact solutions can be used to test the reliability of numerical schemes.

The techniques that are used are motivated by considering two dimensional radially symmetric flows that are produced by injecting water at a varying rate at the axis of symmetry into a region that is initially filled with oil. The injection process produces an expanding circular front separating the oil filled region ahead from a 'mushy' region behind that contains both oil and water. At large times the flow in the vicinity of the front 'forgets' the details of the injection process and becomes self-similar. In particular, the strength of the front, which is measured by the value of the water saturation behind it, asymptotes to a constant value. The self-similar flows described in this paper are not radially symmetric, even though there is a constant strength front separating the oil filled region ahead from the mushy region behind. The solutions are not valid inside the region where the fluid is injected; there the flow is extremely complicated and depends upon the detailed nature of the injection process. Rather, the effect of the flow in the injection region on that outside is modeled by specifying the shape of a contour of constant water saturation. Once this iso-saturation contour is specified at some reference time, its subsequent motion, together with the flow ahead of it, is uniquely determined. Only when this contour is a circle is the flow radially symmetric.

Mainly, for definiteness, this paper describes self-similar flows of two-phase fluids when the region ahead of the front contains a single phase. However, as is indicated in § 11, the solutions can be generalized to study self-similar flows of multi-phase fluids.

Flows in a porous medium have many similarities to flows in Hele-Shaw cells. When the fluids involved are Newtonian, so that the mean flow is governed by Laplace's equation, there are many well developed mathematical techniques that have been used to study such flows. In the seminal papers of Saffman & Taylor (1958) and Taylor (1961), hodograph techniques were used to construct solutions describing steady fingering flows. These solutions were generalized by Alexandrou & Entov (1997) to describe fingering flows of non-Newtonian fluids. Much of the recent research on unsteady Hele-Shaw cell flows of Newtonian fluids, notably by Howison, Ockendon & Lacey (1985), Howison (1986) and Entov & Etingof (1997), is based on complex variable techniques that were developed by Richardson (1972, 1981). In § 12 it is shown that the techniques used to describe self-similar unsteady flows in a porous medium can be modified to describe self-similar flows that are produced when a viscous fluid is injected into a region containing some other viscous fluid. The fluids may be Newtonian fluids, or non-Newtonian fluids for which the coefficient of viscosity depends on the shear stress.

2 Governing equations

The flows of the immiscible fluids oil and water in an isotropic, homogeneous, matrix are referred to Cartesian axes that are fixed in the matrix. Let s ($0 \leqslant s \leqslant 1$) denote the water saturation, $\mathbf{u}_w, \mathbf{u}_o$ denote the velocities of the water and oil, and p_w, p_o denote the partial pressures in the water and oil. Using standard notation, the governing equations (see Barenblatt, Entov & Ryzhik,1990) are Darcy's law

$$\mathbf{u}_w = -\lambda_w \nabla p_w, \quad \mathbf{u}_o = -\lambda_o \nabla p_o, \tag{2.1}$$

and the mass conservation laws for each component

$$\phi \frac{\partial s}{\partial t} + \nabla \cdot \mathbf{u}_w = 0, \ \phi \frac{\partial (1-s)}{\partial t} + \nabla \cdot \mathbf{u}_o = 0. \tag{2.2}$$

In the simplest Muskat–Leverett model, the mobilities λ_w, λ_o and the capillary pressure

$$p_c = p_o - p_w \tag{2.3}$$

are taken to be known functions of s, and the porosity ϕ is a constant.

If

$$\lambda(s) = \lambda_o + \lambda_w, \ F(s) = \frac{\lambda_w}{\lambda} \ \text{ and } \ \varepsilon(s) = -\frac{\lambda_o \lambda_w}{\lambda} \frac{dp_c}{ds}, \tag{2.4}$$

equations (2.1)–(2.3) imply that s and the bulk velocity

$$\mathbf{u} = \mathbf{u}_w + \mathbf{u}_o \tag{2.5}$$

satisfy the equations

$$\mathbf{u} = -\lambda(s) \nabla p, \ \nabla \cdot \mathbf{u} = 0, \tag{2.6}$$

and

$$\phi \frac{\partial s}{\partial t} + \nabla \cdot (F(s)\mathbf{u} - \varepsilon(s) \nabla s) = 0. \tag{2.7}$$

In terms of $\mathbf{u}$ and s,

$$\mathbf{u}_w = F(s)\mathbf{u} - \varepsilon(s) \nabla s, \tag{2.8}$$

$$\mathbf{u}_o = (1 - F(s))\mathbf{u} + \varepsilon(s) \nabla s; \tag{2.9}$$

in terms of p and s,

$$p_w = p + (F(s) - 1) p_c(s) + \int_s^1 p_c(s) F'(s) ds, \tag{2.10}$$

$$p_o = p + F(s) p_c(s) + \int_s^1 p_c(s) F'(s) ds. \tag{2.11}$$

3 Ideal flows when $p_c = 0$

This paper describes flows in the vicinity of a front as it propagates into an oil filled region. Behind the front there is an annular 'mushy' region containing both oil and water.

https://doi.org/10.1017/S0956792500004289 Published online by Cambridge University Press

When $p_c \neq 0$ equation (2.7) for s is of the convective-diffusive type. However, to the approximation that s is discontinuous at a front, it is consistent to take $p_c = 0$ so that s satisfies a hyperbolic equation. For the unsteady flows discussed here, capillary effects are important only when the saturation gradients are large. For example, they must be considered when the detailed structure of the front is of interest, or when the front focuses to form a caustic.

With $p_c = 0$ and t re-scaled so that ϕt represents time, equation (2.7) simplifies to

$$\frac{\partial s}{\partial t} + \nabla \cdot (F(s)\mathbf{u}) = 0. \tag{3.1}$$

In the oil filled region $s = 0$, and in the mushy region $0 < s < 1$. Typically,

$$\lambda_o = \lambda_o(0)(1-s)^b \text{ and } \lambda_w = \lambda_w(1)s^a, \tag{3.2}$$

where the constants $a, b > 1$. Correspondingly, if μ_w and μ_o denote the viscosities of oil and water and if

$$c = \frac{\lambda_o(0)}{\lambda_w(1)} = \frac{\mu_w}{\mu_o} < 1, \tag{3.3}$$

$$\lambda = \lambda_w(1)(s^a + c(1-s)^b) \text{ and } F = \frac{s^a}{s^a + c(1-s)^b}. \tag{3.4}$$

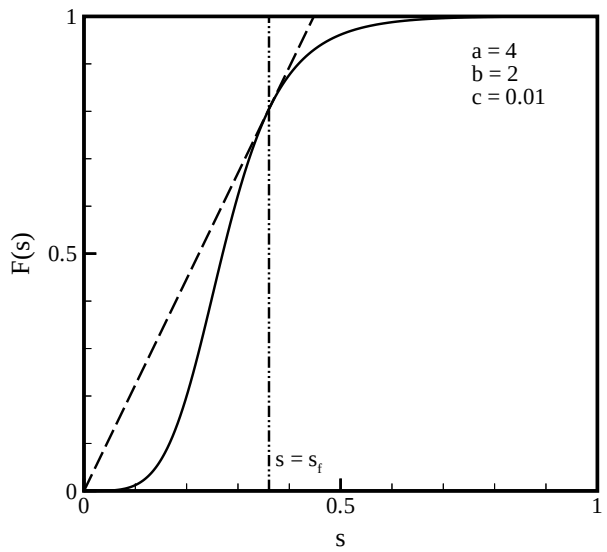

FIGURE 1. Typical form of $F(s)$. s_f denotes the saturation behind the front.

In practice, $\lambda_w = 0$ for $0 \leqslant s \leqslant s_m < 1$ and $\lambda_o = 0$ for $s_M \leqslant s < 1$, where s_m and s_M are experimentally determined constants with $s_m < s_M$. In this paper, we take $s_m = 0$ and $s_M = 1$: any other choices for these constants simply complicates the algebra. The general representations are valid for any form of the dependence of the mobilities on the

https://doi.org/10.1017/S0956792500004289 Published online by Cambridge University Press

saturation. The profile of $F(s)$ for typical values (a, b, c) is shown in Figure 1. Note that

$$F(0) = 0,\ F(1) = 1 \quad \text{and that} \quad F'(0) = F'(1) = 0. \tag{3.5}$$

At a front s is discontinuous, but p and the component of $\mathbf{u}$ normal to the front are continuous. Also, there is a condition that follows from the fact that the mass of each phase is conserved at the passage of the front. If $t = w(\mathbf{x})$ denotes the arrival time of a front at $\mathbf{x}$ and if $[s]$ and $[F(s)]$ denote the jumps in s and $F(s)$ at its passage, this condition requires that

$$\frac{[s]}{[F(s)]} = \mathbf{u} \cdot \nabla w. \tag{3.6}$$

Since condition (3.6) involves only the component of $\mathbf{u}$ normal to the front, $\mathbf{u}$ can be evaluated either ahead or behind the front. This paper is concerned mainly with fronts moving into oil filled region where $s = F(s) = 0$. Then

$$\frac{[s]}{[F(s)]} = \frac{s}{F(s)}, \tag{3.7}$$

where the right-hand side is evaluated behind the front.

4 Motivation: Radially symmetric flows

This first study describes *two dimensional* unsteady *self-similar* flows that are generated by injecting water at a varying rate into a region that is initially filled with oil. The procedures that are used are best motivated by considering the idealized case of radially symmetric flows that are produced by a source of varying strength situated at the origin. If $R(t)$ represents the radial position at time t of particles that were located at the origin at $t = 0$, for all radially symmetric flows the second of conditions (2.6) implies that the radial velocity

$$q = R(t)R'(t)/r. \tag{4.1}$$

The source is of strength $2\pi R(t)R'(t)$. According to (3.1) and (4.1), in the mushy region $s(t, r)$ satisfies the Buckley–Leverett simple wave equation

$$\frac{\partial s}{\partial t} + F'(s)\frac{R(t)R'(t)}{r}\frac{\partial s}{\partial r} = 0, \tag{4.2}$$

$$\text{or } \frac{1}{R}\frac{\partial s}{\partial R} + F'(s)\frac{1}{r}\frac{\partial s}{\partial r} = 0. \tag{4.3}$$

At the front, where $t = w(r)$ and $R = R(w(r)) = W(r)$, (3.6), (3.7) and (4.1) imply

$$\frac{s}{F(s)} = \frac{W}{r}\frac{dW}{dr}. \tag{4.4}$$

Figures 2(a) and 2(b) show a typical development in the s versus r profiles with increasing R, together with the corresponding s and R versus r profiles at the front, that are predicted by equations (4.3) and (4.4). These profiles are obtained using procedures that are standard in the study of gas dynamics (see Whitham, 1974). The illustrations

https://doi.org/10.1017/S0956792500004289 Published online by Cambridge University Press

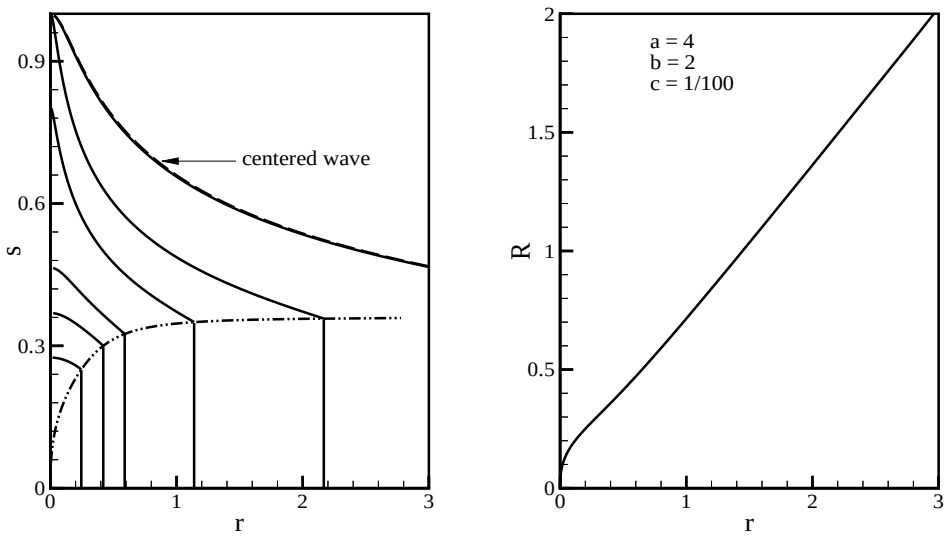

FIGURE 2. (a) A typical development of the saturation profile with increasing R in a radially symmetric flow. The broken curve depicts the variation of the saturation behind the front with radial distance. (b) The corresponding trajectory of the front.

correspond to the simple case when $s(0, r) = 0$ and

$$s(t, 0) = \begin{cases} R/R_0 \text{ for } 0 \leqslant R \leqslant R_0 \\ 1 \text{ for } R \geqslant R_0. \end{cases} \quad . \tag{4.5}$$

The corresponding injection process first produces a compression wave followed by an expansion wave. At $r = 0$ the change from compression to expansion occurs when $R/R_0 = s_I$, where $F''(s_I) = 0$. The front forms at $r = 0$ when $t = 0$ and $s = 0$. Thereafter, at the front s increases monotonically with increasing R and as $R/R_0 \to \infty$ asymptotes to a maximum value s_f that satisfies the condition (see Figure 1):

$$F'(s_f) = \frac{F(s_f)}{s_f}. \tag{4.6}$$

The dependence of s_f on the parameters a, b, c is shown in Figure 3.

Figures 2(a) and 2(b) also compare the s versus r profiles with that in the expansion wave that is centered at $(r, R) = (0, R_0)$. In this wave, depicted by the broken curve,

$$F'(s) = \frac{r^2}{R^2 - R_0^2}. \tag{4.7}$$

With $s(r, R)$ determined by (4.7), at the front

$$r^2(F(s)/F'(s) - s) = \text{constant}. \tag{4.8}$$

Equations (4.7) and (4.8), which determine the trajectory of the front, are uniformly valid in the mushy region where $s > s_I$ and $R > R_0$. In the limit as $R/R_0 \to \infty$, the flow 'forgets'

https://doi.org/10.1017/S0956792500004289 Published online by Cambridge University Press

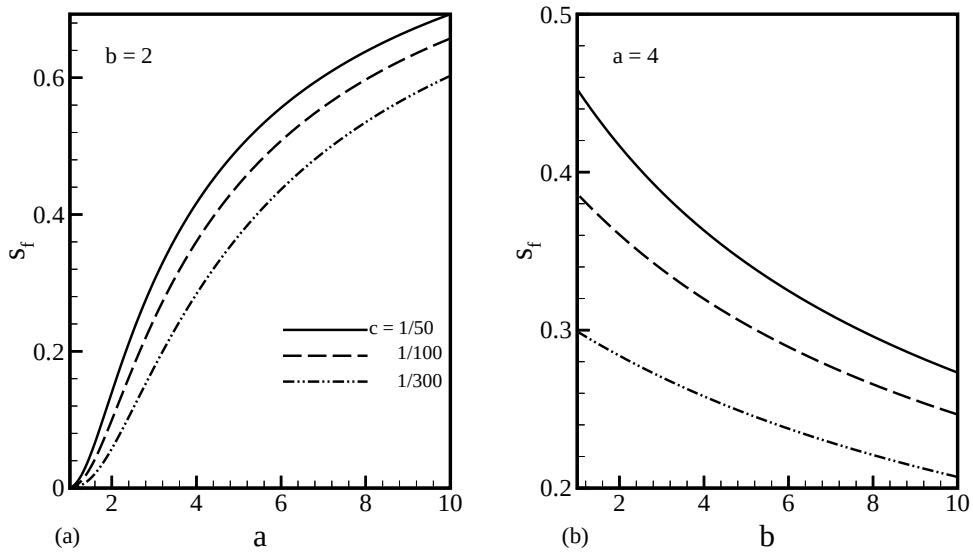

FIGURE 3. The dependence of s_f on the parameters a, b, c.

details of the injection process and asymptotes to the self-similar flow in which

$$F'(s) = \frac{r^2}{R^2} \tag{4.9}$$

and

$$q = R'(t)\frac{R}{r} = \frac{R'(t)}{\sqrt{F'(s)}}. \tag{4.10}$$

These relations are valid throughout the mushy region where $s_f \leqslant s \leqslant 1$. At the expanding circular front q and p are continuous:

$$q, = q_f, = R'(t)Q_f \quad \text{where} \quad Q_f = (F'(s_f))^{-1/2} < 1, \tag{4.11}$$

and, without loss of generality, $p = 0$. In the mushy region, with $s(r, R)$ determined by (4.9),

$$p = -\frac{1}{2}R(t)R'(t)\int_{s_f}^{s} \frac{F''(s)}{\lambda(s)F'(s)}ds; \tag{4.12}$$

and in the oil filled region, with

$$q = R'(t)\frac{R}{r},\ p = \frac{R(t)R'(t)}{\lambda(0)}\ln(q/q_f). \tag{4.13}$$

4.1 Remark

Note that if

$$q = R'(t)Q(R, r), \tag{4.14}$$

https://doi.org/10.1017/S0956792500004289 Published online by Cambridge University Press

then in both the mushy and the oil filled regions $Q = R/r$ satisfies the equation

$$Q\frac{\partial Q}{\partial R} + \frac{\partial Q}{\partial r} = 0. \tag{4.15}$$

In the mushy region, where $Q > Q_f$, $s = S(Q)$ and $\lambda = \Lambda(Q)$ are determined from the conditions

$$F'(s) = 1/Q^2,\ \Lambda = \lambda_o(s) + \lambda_w(s). \tag{4.16}$$

In the oil filled region, where $Q < Q_f$,

$$S(Q) = 0 \ \text{ and } \ \Lambda(Q) = \lambda_o(0). \tag{4.17}$$

In both regions

$$p = R'(t)R(t)\int_{Q_f}^{Q} \frac{dQ'}{\Lambda(Q')Q'}. \tag{4.18}$$

5 Generalized self-similar flows

When the radially symmetric flow behind a circular front is self-similar, the strength of the front, $[s]$, is constant. This paper describes other self-similar flows behind *non-circular,* constant strength, fronts whose shapes at any reference time can be specified *arbitrarily*. The fronts are produced by injecting water into a region near the origin of typical dimension r_0 at a rate $2\pi r_0^2 R(t)R'(t)$. Let $(x,\ y)$ be measured in units of r_0 and (u, v) in units of $r_0 R'(t)$. Also, if $\bar{\lambda}$ denotes some reference value of the bulk mobility, let p be measured in units of $r_0^2 R'(t)/\bar{\lambda}$ and λ in units of $\bar{\lambda}$.

Using (x, y, R) rather than (x, y, t) as the independent variables, for *any* two dimensional flow equations (2.6) imply

$$u = Q\cos\beta = -\lambda\frac{\partial p}{\partial x} = \frac{\partial \psi}{\partial y}, \tag{5.1}$$

$$v = Q\sin\beta = -\lambda\frac{\partial p}{\partial y} = -\frac{\partial \psi}{\partial x}. \tag{5.2}$$

In (5.1) and (5.2), $r_0^2 R'(t)\psi$ is the streamfunction, $r_0 R'(t)Q$ is the fluid speed, and β is the flow angle. ψ changes by $2\pi R(t)$ around any closed curve surrounding the injection region. Equation (3.1) becomes

$$\frac{\partial s}{\partial R} + \frac{\partial (F(s)u)}{\partial x} + \frac{\partial (F(s)v)}{\partial y} = 0, \tag{5.3}$$

or, using the second of equations (2.6),

$$\frac{\partial s}{\partial R} + F'(s)\left(u\frac{\partial s}{\partial x} + v\frac{\partial s}{\partial y}\right) = 0. \tag{5.4}$$

These equations are valid *outside* a simply connected region near the origin where fluid is injected.

If $R = W(x, y)$ is the equation of a front, the unit normal to the front is

$$\nabla W / |\nabla W| = (\cos\theta, \sin\theta), \tag{5.5}$$

https://doi.org/10.1017/S0956792500004289 Published online by Cambridge University Press

say. The conditions that the normal component of velocity and that the tangential derivative of p are continuous then imply

$$[Q\cos(\theta-\beta)]=0 \quad \text{and} \quad [(Q/\lambda)\sin(\theta-\beta)]=0. \tag{5.6}$$

Additionally, according to (3.6)

$$\frac{[s]}{[F(s)]}=Q\left(\cos\beta\frac{\partial W}{\partial x}+\sin\beta\frac{\partial W}{\partial y}\right)=Q\cos(\theta-\beta)\,|\nabla W|\,. \tag{5.7}$$

In view of the first of conditions (5.6), in (5.7) Q and β can be evaluated either behind or ahead of the front.

With $\lambda(s)$ and $F(s)$ specified, equations (5.1) and (5.4) yield *five* conditions for the *five* unknowns Q, β, p, ψ and s. For the special case of self-similar flows described in this paper, these conditions are supplemented by the conditions that

$$s=S(Q) \text{ and } \lambda=\Lambda(Q), \tag{5.8}$$

where $S(Q)$ and $\Lambda(Q)$ are determined from the parametric relations (4.16) and (4.17). It follows from the first of (4.16), (5.4) and (5.8) that in the mushy region $Q(R,x,y)$ satisfies the equation

$$Q\frac{\partial Q}{\partial R}+\cos\beta\frac{\partial Q}{\partial x}+\sin\beta\frac{\partial Q}{\partial y}=0. \tag{5.9}$$

For the self-similar flows discussed here this equation holds also in the oil filled region. When the flow is radially symmetric, (5.9) reduces to (4.15).

With s and λ given by (5.8), equations (5.1) and (5.9) yield *five* conditions for the *four* unknown functions Q, β, p and ψ. In the following section it is shown that these equations are compatible.

6 Transformation to hodograph variables

Only flows in which Q and β vary independently are considered. With

$$G=\frac{Q}{\Lambda(Q)} \text{ and } C=-\left(\frac{1}{\Lambda(Q)}+\int_{Q_f}^{Q}\frac{dQ'}{\Lambda(Q')Q'}\right), \tag{6.1}$$

all of the equations (5.1) and (5.9) are satisfied by expressions of the form

$$p=-G(Q)(x\cos\beta+y\sin\beta)-RC(Q)+P(Q,\beta) \tag{6.2}$$

and

$$\psi=Q(-x\sin\beta+y\cos\beta)+\beta R+\Psi(Q,\beta). \tag{6.3}$$

These representations are motivated by results obtained by Cumberbatch & Varley (1966) in their research on shock waves in gases. Equations (5.1) and (6.2) yield the conditions

$$G'(Q)(x\cos\beta+y\sin\beta)+RC'(Q)=\frac{\partial P}{\partial Q}, \tag{6.4}$$

$$G(Q)(-x\sin\beta+y\cos\beta)=\frac{\partial P}{\partial\beta}; \tag{6.5}$$

https://doi.org/10.1017/S0956792500004289 Published online by Cambridge University Press

equations (5.1) and (6.3) yield the conditions

$$x \sin\beta - y \cos\beta = \frac{\partial \Psi}{\partial Q}, \tag{6.6}$$

and

$$Q(x \cos\beta + y \sin\beta) - R = \frac{\partial \Psi}{\partial \beta}. \tag{6.7}$$

Since, by (6.1),

$$QC'(Q) + G'(Q) = 0, \tag{6.8}$$

equations (6.4)–(6.7) are compatible if $\Psi(Q, \beta)$ and $P(Q, \beta)$ satisfy the equations

$$G(Q)\frac{\partial \Psi}{\partial Q} = -\frac{\partial P}{\partial \beta} \text{ and } G'(Q)\frac{\partial \Psi}{\partial \beta} = Q\frac{\partial P}{\partial Q}. \tag{6.9}$$

It remains to prove that equation (5.9) is satisfied. This can be re-written as

$$Q\frac{\partial(Q, x, y)}{\partial(R, x, y)} - \cos\beta\frac{\partial(Q, R, y)}{\partial(R, x, y)} + \sin\beta\frac{\partial(Q, R, x)}{\partial(R, x, y)} = 0. \tag{6.10}$$

If (x, y) are regarded as functions of (R, Q, β), (6.10) implies

$$Q\frac{\partial(Q, x, y)}{\partial(R, Q, \beta)} - \cos\beta\frac{\partial(Q, R, y)}{\partial(R, Q, \beta)} + \sin\beta\frac{\partial(Q, R, x)}{\partial(R, Q, \beta)} = 0, \tag{6.11}$$

or

$$Q\frac{\partial(x, y)}{\partial(\beta, R)} + \cos\beta\frac{\partial y}{\partial \beta} - \sin\beta\frac{\partial x}{\partial \beta} = 0, \tag{6.12}$$

or

$$\left(\cos\beta - Q\frac{\partial x}{\partial R}\right)\frac{\partial y}{\partial \beta} + \left(Q\frac{\partial y}{\partial R} - \sin\beta\right)\frac{\partial x}{\partial \beta} = 0. \tag{6.13}$$

Since $\Psi = \Psi(\beta, Q)$, equations (6.6) and (6.7) yield

$$Q\frac{\partial x}{\partial R} = \cos\beta,\ Q\frac{\partial y}{\partial R} = \sin\beta, \tag{6.14}$$

and (6.13) is trivially satisfied.

The radially symmetric flows discussed in the previous section correspond to the trivial choices

$$x = r\cos\beta,\ y = r\sin\beta,\ Q = R/r, P = \Psi = 0.$$

7 Constant strength fronts

The self-similar flows described in the previous section can occur behind a constant strength front that propagates with normal speed $r_0 R'(t) Q_f^{-1}$ into an oil filled region. The constant Q_f is determined from (4.6) and (4.11). Since $[Q] = 0$ but $[A] \neq 0$, conditions (5.6) imply that at the front the flow angle β is continuous and equal to θ, so that the flow directions ahead and behind are always normal to the front. The fluid speed at the front is $r_0 R'(t) Q_f$, which is less than the speed of the front.

https://doi.org/10.1017/S0956792500004289 Published online by Cambridge University Press

Let

$$R = W(x, y) \tag{7.1}$$

denote the trajectory of the front. With Q_f given by (4.11), (5.7) implies that $W(x, y)$ satisfies the equation

$$\cos\beta \frac{\partial W}{\partial x} + \sin\beta \frac{\partial W}{\partial y} = Q_f. \tag{7.2}$$

Let

$$A(\beta) = \frac{\partial \Psi(Q_f, \beta)}{\partial \beta} \quad \text{and} \quad B(\beta) = \frac{\partial \Psi(Q_f, \beta)}{\partial Q}. \tag{7.3}$$

Then, according to (6.6) and (6.7), with $\beta(x, y)$ determined from the condition

$$x \sin\beta - y \cos\beta = B(\beta), \tag{7.4}$$

at the front

$$R = Q_f(x \cos\beta + y \sin\beta) - A(\beta) = W(x, y). \tag{7.5}$$

These conditions, together with the conditions that Q and β are continuous, imply that $A(\beta)$ and $B(\beta)$ are continuous at the front.

Equations (7.4) and (7.5) imply that at the front

$$\frac{\partial W}{\partial x} = Q_f \cos\beta - (A'(\beta) + Q_f B(\beta)) \frac{\partial \beta}{\partial x}, \tag{7.6}$$

$$\frac{\partial W}{\partial y} = Q_f \sin\beta - (A'(\beta) + Q_f B(\beta)) \frac{\partial \beta}{\partial y}, \tag{7.7}$$

and

$$\cos\beta \frac{\partial \beta}{\partial x} + \sin\beta \frac{\partial \beta}{\partial y} = 0. \tag{7.8}$$

Consequently, equation (7.2) is satisfied for any choices of the functions $A(\beta)$ and $B(\beta)$.

$A(\beta)$ and $B(\beta)$ are not independent functions. The condition that $\beta = \theta$ at the front implies that

$$A'(\beta) + Q_f B(\beta) = 0, \tag{7.9}$$

a result that follows by using relations (7.4), (7.5) and the condition that at constant R

$$\frac{dy}{dx} \tan\beta = -1. \tag{7.10}$$

Using (7.4), (7.5) and (7.9), the equation of the front is given parametrically as

$$Q_f x = (R + A(\beta)) \cos\beta - A'(\beta) \sin\beta, \tag{7.11}$$

$$Q_f y = (R + A(\beta)) \sin\beta + A'(\beta) \cos\beta, \tag{7.12}$$

or, with $z = x + iy$, as

$$Q_f z = (R + A(\beta) + iA'(\beta)) e^{i\beta}. \tag{7.13}$$

https://doi.org/10.1017/S0956792500004289 Published online by Cambridge University Press

According to (6.3), (6.6) and (6.7),

$$\psi = \Psi - Q\frac{\partial \Psi}{\partial Q} + \beta R, \tag{7.14}$$

so, in particular, at the front

$$\frac{\partial \psi}{\partial \beta} = A''(\beta) + A(\beta) + R = \rho, \tag{7.15}$$

where ρ denotes the radius of curvature of the front.

As for the case of radially symmetric flows, in what follows p can be measured so that $p = 0$ at the front. To show that p is independent of β at the front, first note that (6.2), (6.6) and (6.7) imply that

$$p = R\int_{Q_f}^{Q} \frac{dQ'}{\Lambda(Q')Q'} + P - \Lambda^{-1}\frac{\partial \Psi}{\partial \beta}. \tag{7.16}$$

Consequently, at any constant R and Q

$$\frac{\partial p}{\partial \beta} = \frac{\partial P}{\partial \beta} - \Lambda^{-1}\frac{\partial^2 \Psi}{\partial \beta^2} = -\Lambda^{-1}\left(Q\frac{\partial \Psi}{\partial Q} + \frac{\partial^2 \Psi}{\partial \beta^2}\right). \tag{7.17}$$

In particular, using (7.3) and (7.9), at the front

$$\frac{\partial p}{\partial \beta} = -\frac{1}{\Lambda(Q_f)}(A'(\beta) + Q_f B(\beta)) = 0. \tag{7.18}$$

In (7.11) and (7.12), the function $A(\beta)$ can be determined in terms of the shape of the front at some reference time when $R = R_0$. For example, when the front is the ellipse

$$\frac{x^2}{(1+m)^2} + \frac{y^2}{(1-m)^2} = 1, \tag{7.19}$$

$$A + R_0 = Q_f(1+m)(1 - 4m\sin^2\beta/(1+m)^2)^{1/2}. \tag{7.20}$$

More generally, if $r = g(\theta)$ is the polar equation of the front at $R = R_0$, $A(\beta)$ is determined parametrically from the conditions that

$$A + R_0 = Q_f g(\theta)\cos(\theta - \beta) \quad \text{and} \quad \tan(\theta - \beta) = g'(\theta)/g(\theta). \tag{7.21}$$

These relations follow from (7.13) with $z = g(\theta)e^{i\theta}$.

8 Problem for $\Psi(\beta, Q)$

Eliminating P from equations (6.9) and using (6.8) yields the equation

$$Q^2\frac{\partial^2 \Psi}{\partial Q^2} + K(Q)\left(Q\frac{\partial \Psi}{\partial Q} + \frac{\partial^2 \Psi}{\partial \beta^2}\right) = 0, \tag{8.1}$$

where

$$K(Q) = 1 - Q\frac{\Lambda'(Q)}{\Lambda(Q)}. \tag{8.2}$$

https://doi.org/10.1017/S0956792500004289 Published online by Cambridge University Press

Equation (8.1) must be solved subject to the conditions that

$$\text{when } Q = Q_f, \ \frac{\partial \Psi}{\partial \beta} = A(\beta) \ \text{ and } \ Q_f \frac{\partial \Psi}{\partial Q} = -A'(\beta). \tag{8.3}$$

In terms of $\Psi(Q, \beta)$,

$$x = \frac{\partial \Psi}{\partial Q} \sin\beta + Q^{-1} \left(R + \frac{\partial \Psi}{\partial \beta} \right) \cos\beta \tag{8.4}$$

$$y = -\frac{\partial \Psi}{\partial Q} \cos\beta + Q^{-1} \left(R + \frac{\partial \Psi}{\partial \beta} \right) \sin\beta, \tag{8.5}$$

or, using complex notation,

$$z = Q^{-1} e^{i\beta} \left(R + \frac{\partial \Psi}{\partial \beta} - iQ \frac{\partial \Psi}{\partial Q} \right). \tag{8.6}$$

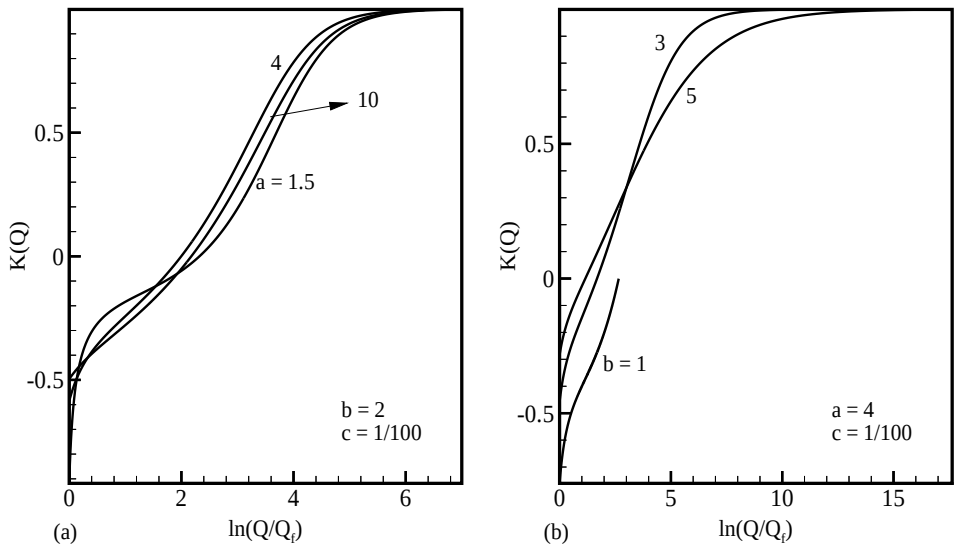

FIGURE 4. $K(Q)$ for typical values of a, b, c.

In what follows, we consider flows in which $Q > Q_f$ in the mushy region and $Q < Q_f$ in the oil filled region. Figure 4 shows a typical form of $K(Q)$ in the mushy region. With Q_c determined from the condition that $K(Q_c) = 0$, behind the front $K < 0$ for $Q_f \leqslant Q < Q_c$ and $K > 0$ for $Q > Q_c$. Consequently, (8.1) is a hyperbolic equation when $Q_f \leqslant Q < Q_c$ and an elliptic equation when $Q > Q_c$. In the oil filled region $K(Q) \equiv 1$ and Ψ satisfies the elliptic equation

$$Q^2 \frac{\partial^2 \Psi}{\partial Q^2} + Q \frac{\partial \Psi}{\partial Q} + \frac{\partial^2 \Psi}{\partial \beta^2} = 0. \tag{8.7}$$

https://doi.org/10.1017/S0956792500004289 Published online by Cambridge University Press

8.1 Singularities

A flow that has bounded saturation gradients at $t = 0$ may develop in a finite time into a flow that has unbounded gradients. Such singularities occur when

$$\frac{\partial(x, y)}{\partial(Q, \beta)} = 0, \tag{8.8}$$

which requires that

$$K^{-1}\left(Q^2\frac{\partial^2\Psi}{\partial Q^2}\right)^2 + \left(Q\frac{\partial^2\Psi}{\partial Q\partial\beta} - \frac{\partial\Psi}{\partial\beta} - R\right)^2 = 0. \tag{8.9}$$

This condition is identical to that which holds when some contour of constant saturation develops a cusp. In the elliptic region where $K > 0$, (8.9) can only be satisfied at a time when

$$R = Q\frac{\partial^2\Psi}{\partial Q\partial\beta} - \frac{\partial\Psi}{\partial\beta} \tag{8.10}$$

if Q and β are restricted by the condition

$$\frac{\partial^2\Psi}{\partial Q^2} = 0. \tag{8.11}$$

Condition (8.11) is satisfied at all points of the front and condition (8.10) is satisfied when

$$R = -(A''(\beta) + A(\beta)) = -\rho_0(\beta), \tag{8.12}$$

where $\rho_0(\beta)$ denotes the radius of curvature when $R = 0$. Consequently, the front develops a cusp only when it contains a dimple.

Singularities may develop in the hyperbolic region behind the front where $K < 0$. Since the saturation gradients become large as such singularities form, capillary effects that are modeled by the term $\varepsilon(s)\nabla s$ in equations (2.8) and (2.9) become locally important.

9 Flows in unbounded regions

When the region occupied by the fluid is unbounded, $A(\beta)$ can be expanded in a Fourier series as

$$A(\beta) = A_0 + \sum_{n=1} (A_n\cos(n\beta) + B_n\sin(n\beta)), \tag{9.1}$$

or, using complex notation with $C_n = A_n + iB_n$,

$$A(\beta) = A_0 + \mathrm{Re}\left[\sum_{n=1} C_n e^{-in\beta}\right]. \tag{9.2}$$

The corresponding solution to (8.1) can be written as

$$\Psi = A_0\beta + \sum_{n=1} n^{-1}(A_n\sin(n\beta) - B_n\cos(n\beta))\Psi_n(Q),$$

$$= A_0\beta - \mathrm{Im}\left[\sum_{n=1} n^{-1}C_n e^{-in\beta}\Psi_n(Q)\right], \tag{9.3}$$

https://doi.org/10.1017/S0956792500004289 Published online by Cambridge University Press

where the $\Psi_n(Q)$ satisfy the equation

$$Q^2\Psi_n'' + K(Q)(Q\Psi_n' - n^2\Psi_n) = 0 \tag{9.4}$$

with

$$\Psi_n(Q_f) = 1 \text{ and } Q_f\Psi_n'(Q_f) = n^2. \tag{9.5}$$

In the oil filled region

$$\Psi_n(Q) = \frac{1}{2}(1+n)\left(\frac{Q}{Q_f}\right)^n - \frac{1}{2}(n-1)\left(\frac{Q}{Q_f}\right)^{-n}. \tag{9.6}$$

In the mushy region the $\Psi_n(Q)$ must be determined numerically.

Using the representation (9.3) for Ψ, the expressions (8.6) can be written

$$z = Q^{-1}e^{i\beta}\left(R + A_0 + \frac{1}{2}\sum_{n=1}\left[C_n(\Psi_n + n^{-1}Q\Psi_n')e^{-in\beta} + \overline{C}_n(\Psi_n - n^{-1}Q\Psi_n')e^{in\beta}\right]\right). \tag{9.7}$$

Since $\Psi_1(Q) = Q/Q_f$, in (9.7) the constants A_0 and C_1 can be taken to be zero; non-zero values correspond to shifts in the origins of R, x and y. With Ψ given by (9.3), (7.14) and (7.16) imply

$$\psi = \beta R + \operatorname{Im}\left[\sum_{n=2} n^{-1}C_n(Q\Psi_n' - \Psi_n)e^{-in\beta}\right], \tag{9.8}$$

and

$$p = R\int_{Q_f}^{Q}\frac{dQ'}{\Lambda(Q')Q'} + \Lambda^{-1}\operatorname{Re}\left[\sum_{n=2} C_n(n^{-2}Q\Psi_n' - \Psi_n)e^{-in\beta}\right]. \tag{9.9}$$

Since the streamfunction is $r_0^2R'(t)\psi$, the flow rate across any closed curve that surrounds the origin is $2\pi r_0^2R(t)R'(t)$.

In the oil filled region the flow is potential flow and the expressions (9.7)–(9.9) can be simplified by introducing the complex variable ζ through the relation

$$u - iv = Qe^{-i\beta} = Q_f\zeta^{-1}. \tag{9.10}$$

Then

$$z(\zeta, R) = Q_f^{-1}\left(R\zeta + \frac{1}{2}\sum_{n=2}((n+1)C_n\zeta^{(1-n)} - (n-1)\overline{C}_n\zeta^{(n+1)})\right), \tag{9.11}$$

and the complex potential

$$\Phi(\zeta, R) = -\lambda_o(0)p + i\psi = R\log\zeta + \frac{1}{2}\sum_{n=2} n^{-1}(n^2-1)(C_n\zeta^{-n} - \overline{C}_n\zeta^n). \tag{9.12}$$

It follows that

$$u - iv = \frac{\partial\Phi}{\partial\zeta}\Big/\frac{\partial z}{\partial\zeta}. \tag{9.13}$$

Although it is tempting to try to determine the flow in both the mushy and the oil filled regions in terms of the shape of the front at $R = R_0$, this problem is ill-posed! By

https://doi.org/10.1017/S0956792500004289 Published online by Cambridge University Press

the time that the strength of the front has stopped changing, its shape is almost circular even when the flow in the mushy region well behind the front is far from being radially symmetric. In what follows we describe flows in the mushy region between the front and an inner surface, S_0, on which the saturation s is a specified constant, $= s_0$. A well-posed problem is that of determining the flow in this annular region in terms of its shape when $R = R_0$. Of particular interest is the case when the saturation s_0 is close to unity, so that the inner surface is almost stationary when compared to the motion of the front. In this limit, the front is almost circular even when S_0 is far from circular.

According to (9.7), with

$$Q_0 = (F'(s_0))^{-1/2},\ m_n = \Psi_n(Q_0)C_n \text{ and } \gamma_n = \frac{Q_0\Psi_n'(Q_0)}{n\Psi_n(Q_0)}, \tag{9.14}$$

the parametric representation for S_0 is given by

$$z = Q_0^{-1}e^{i\beta}\left(R + \frac{1}{2}\sum_{n=2}((1+\gamma_n)m_n e^{-in\beta} + (1-\gamma_n)\overline{m}_n e^{in\beta})\right). \tag{9.15}$$

In general, once s_0 and S_0 have been specified, the real constants γ_n and the complex constants m_n must be determined numerically. However, in the limit $Q_0 \to Q_f$

$$\gamma_n(Q_0) \to n \text{ and } m_n \to C_n. \tag{9.16}$$

The problem of determining the m_n simplifies also in the important limit as $s_0 \to 1$, $(Q_0 \to \infty)$. Since $K(Q)$ given by (8.2) tends to 1, and since the solution to (9.4) $\Psi_n(Q) \propto Q^n$ as $Q \to \infty$, as $s_0 \to 1$

$$\gamma_n(Q_0) \to 1. \tag{9.17}$$

Thus, to a first approximation, at S_0

$$z = Q_0^{-1}e^{i\beta}\left(R + \sum_{n=2} m_n e^{-in\beta}\right), \tag{9.18}$$

or, with $\xi = e^{i\beta}$,

$$z = Q_0^{-1}\xi\left(R + \sum_{n=2} m_n \xi^{-n}\right). \tag{9.19}$$

Consequently, *the complex constants m_n are determined by the conformal mapping that maps the exterior of the unit circle in the complex ξ-plane onto the region exterior to S_0 in the complex z-plane.*

As a simple application of the representation (9.19), suppose S_0 is an ellipse at $R = R_0$ with a ratio of minor to major axes of $(1-m)/(1+m)$. Then, with $m_2 = R_0 m$ and $m_n = 0$ for $n > 2$, (9.19) reduces to

$$z = R_0 Q_0^{-1}((R/R_0)\xi + m\xi^{-1}), \tag{9.20}$$

which represents an ellipse whose ratio of minor to major axes at any R is $(R - mR_0)/(R + mR_0)$. As $(R/R_0) \to \infty$, S_0 tends to a circle. Figures 5(a) and 5(b) show the s, p and ψ contours at $R = R_0$ when $m = 0.975$ and $s_0 = 0.9995$. Since the $\gamma_n\ (Q_0) \simeq 1$ at this value of s_0, equation (9.15) for S_0 is only approximated by (9.20). When S_0 is constrained to be

https://doi.org/10.1017/S0956792500004289 Published online by Cambridge University Press

exactly an ellipse at $R = R_0$, more than a single mode must be used in the representation (9.15). The corresponding values of the m_n are found by a straightforward iteration process. Of course, with a value of s_0 so close to one, the effect of these higher order modes is insignificant. However, for smaller values of s_0 the higher modes are important. As an example, Figures 6(a) and 6(b) show the s, p and ψ contours when s_0 is close to s_f. For this flow S_0 is not specified a priori but is determined from the condition that the series (9.7) contains a finite number of terms. In the illustration, only four of the complex constants m_n are non-zero. Figures 7(a) and 7(b) show the s, p and ψ contours when s_0 is close to unity and four modes are excited.

10 The flow down a wedge

As a second application of the representations obtained above, consider flows that are produced by injecting water at a rate $\beta_0 r_0^2 R(t)R'(t)$ in some vicinity of the apex of a wedge of angle β_0 (see Figures 8(a) and 8(b)). If the rigid boundaries of the wedge are the lines

$$y = 0 \quad \text{and} \quad y = \tan(\beta_0)x, \tag{10.1}$$

(7.11), (7.12) and the condition that these boundaries are streamlines for all R requires that

$$\frac{\partial \Psi}{\partial Q} = 0 \quad \text{when} \quad \beta = 0 \quad \text{and} \quad \beta = \beta_0. \tag{10.2}$$

Then, by (8.3),

$$A'(0) = A'(\beta_0) = 0, \tag{10.3}$$

and $A(\beta)$ can be expanded in a Fourier series as

$$A(\beta) = \sum_{n=1} A_n \cos(\kappa_n \beta), \text{ where } \kappa_n = n\pi/\beta_0. \tag{10.4}$$

The corresponding representations of z, ψ and p are given by (9.3)–(9.16) with n replaced by κ_n and $C_n = \overline{C}_n = A_n$. Also, in (9.8), (9.9) and (9.15), summation can start with $n = 1$.

11 Multi-phase immiscible fluids

In addition to oil and water phases a fluid may contain several other phases, such as gas phases. When the phases are incompressible and immiscible, the solutions presented above for two phase fluids can be generalized to describe self-similar flows of fluids with n phases. Let $R'(t)(u_i, v_i)$ denote the (x, y) velocity components of the i^{th} phase whose saturation is s_i, and let $R'(t)p$ denote the pressure. When the effect of capillary pressure is neglected, Darcy's law implies that

$$u_i = -\lambda_i \frac{\partial p}{\partial x}, v_i = -\lambda_i \frac{\partial p}{\partial y}, \ i = 1 \cdot \cdot n. \tag{11.1}$$

https://doi.org/10.1017/S0956792500004289 Published online by Cambridge University Press

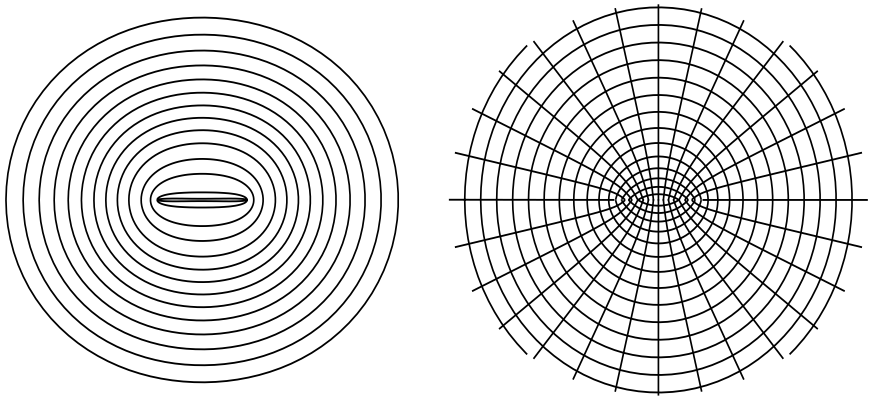

(a) (b)

FIGURE 5. (a) The contours of constant saturation when S_0 is an ellipse. (b) The corresponding streamlines and isobars.

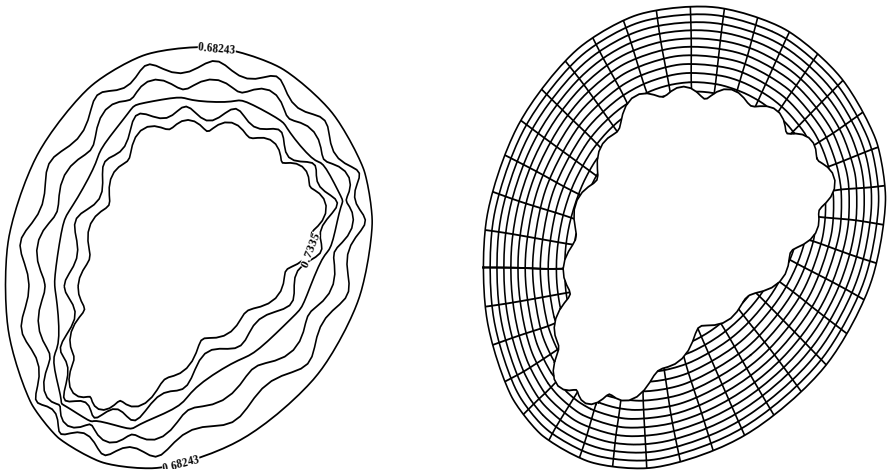

(a) (b)

FIGURE 6. (a) The contours of constant saturation when s_0 is close to s_f and just four nonsequential modes are excited. (b) The corresponding streamlines and isobars.

https://doi.org/10.1017/S0956792500004289 Published online by Cambridge University Press

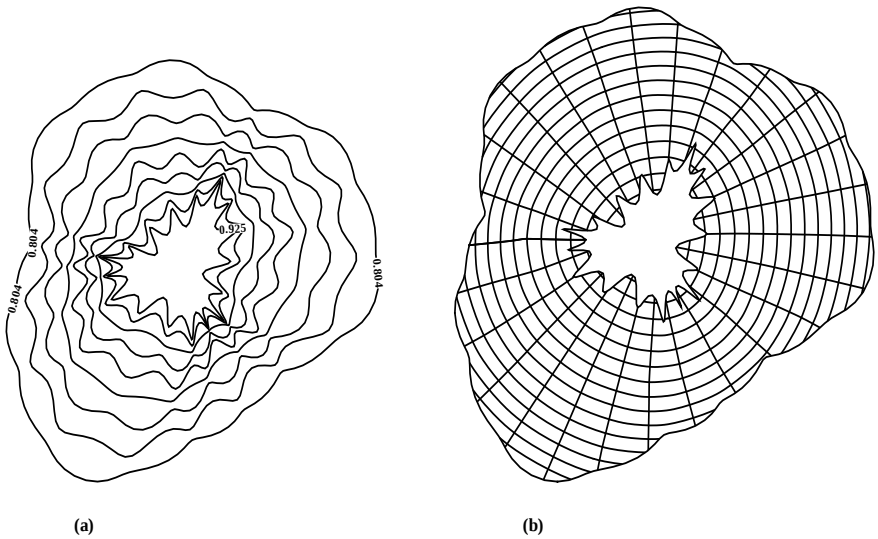

FIGURE 7. (a) The contours of constant saturation when s_0 is close to unity and just four nonsequential modes are excited. (b) The corresponding streamlines and isobars.

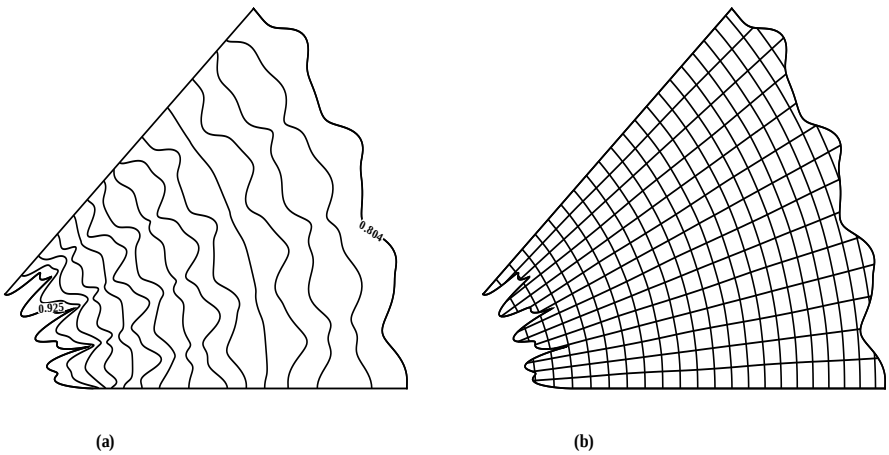

FIGURE 8. (a) The contours of constant saturation in the flow down a wedge. (b) The corresponding streamlines and isobars.

https://doi.org/10.1017/S0956792500004289 Published online by Cambridge University Press

where λ_i denotes the mobility of the i^{th} phase. Additionally, conservation of mass for each phase implies that

$$\frac{\partial s_i}{\partial R} + \frac{\partial u_i}{\partial x} + \frac{\partial v_i}{\partial y} = 0,\ i = 1 \cdot \cdot n. \tag{11.2}$$

Since

$$\sum_{i=1}^{n} s_i = 1, \tag{11.3}$$

in (11.1) the λ_i are regarded as known functions of $(s_1, s_2, \cdot\cdot, s_{n-1})$.

If

$$u = \sum_{i=1}^{n} u_i,\ v = \sum_{i=1}^{n} v_i, \text{ and } \lambda = \sum_{i=1}^{n} \lambda_i, \tag{11.4}$$

by (11.1)–(11.3),

$$u = -\lambda \frac{\partial p}{\partial x}, v = -\lambda \frac{\partial p}{\partial x} \text{ and } \frac{\partial u}{\partial x} + \frac{\partial v}{\partial y} = 0. \tag{11.5}$$

With

$$F_i = \lambda_i/\lambda,\ (u_i, v_i) = F_i(u, v) \tag{11.6}$$

and equations (11.5) are complemented by the $(n-1)$ equations

$$\frac{\partial s_i}{\partial R} + \frac{\partial (uF_i)}{\partial x} + \frac{\partial (vF_i)}{\partial y} = 0,\ i = 1 \cdot \cdot (n-1), \tag{11.7}$$

or, using (11.5), by

$$\frac{\partial s_i}{\partial R} + u\frac{\partial F_i}{\partial x} + v\frac{\partial F_i}{\partial y} = 0,\ i = 1 \cdot \cdot (n-1). \tag{11.8}$$

The F_i satisfy the constraint

$$\sum_{i=1}^{n} F_i = 1. \tag{11.9}$$

Equations (11.5) and (11.8) provide $(n+2)$ equations for the $(n+2)$ unknowns $(u, v, p, s_1, s_2, \cdot\cdot, s_{n-1})$. Across the front $R = W(x, y)$, p and the normal component of the bulk velocity are continuous while

$$\frac{[s_i]}{[F_i]} = u\frac{\partial W}{\partial x} + v\frac{\partial W}{\partial y}. \tag{11.10}$$

11.1 Self-similar flows

For radially symmetric flows, the bulk radial velocity $q = R'(t)R(t)/r$ and equations (11.8) reduce to the system of $(n-1)$ first order partial differential equations

$$\frac{1}{R}\frac{\partial s_i}{\partial R} + \frac{1}{r}\frac{\partial F_i}{\partial r} = 0,\ i = 1 \cdot \cdot (n-1) \tag{11.11}$$

https://doi.org/10.1017/S0956792500004289 Published online by Cambridge University Press

for the $s_i(R,r)$, $i = 1 \cdots (n-1)$. The front conditions (11.10) imply

$$\frac{[s_i]}{[F_i]} = \frac{W}{r}\frac{dW}{dr},\ i = 1 \cdots (n-1). \tag{11.12}$$

Suppose that for $t < 0$ the fluid is at rest with the s_i specified constants, and then at $t = 0$ the (idealized) injection process produces a discontinuous change in the s_i at $r = 0$. When (11.11) form a *completely* hyperbolic system of equations for the $s_i(R,r), i = 1 \cdots (n-1)$, the resulting flow is generated by a system of centered expansion waves that are separated by fronts and regions in which all the s_i are constants. In each such wave $s_i = S_i(Q)$ where $Q = R/r$ and the $S_i(Q)$ satisfy the system of nonlinear ordinary differential equations

$$\left(\frac{\partial F_i}{\partial s_j} - Q^{-2}\delta_{ij}\right) S_j'(Q) = 0,\ (i,j) = 1 \cdots (n-1). \tag{11.13}$$

At a front Q is continuous and

$$\frac{[s_i]}{[F_i]} = Q^2,\ i = 1 \cdots (n-1). \tag{11.14}$$

The pattern of centered waves, fronts, and regions in which the s_i are constant can be quite complex. Consider the simplest case when $n = 2$, so there is at most one centered wave. With $s = s_1$ and $F = F_1$, (11.13) implies that $Q^{-2} = F'(s)$. Let

$$s(0,r) = s_A \text{ for } r > 0 \ \text{ and } \ s(R,0) = \ s_B \text{ for } R > 0, \tag{11.15}$$

where s_A and s_B are constants. Then, there are *three* possible flow patterns. Let $s = s_I$ denote the saturation at which $F(s)$ is inflectional with $F''(s) > 0$ for $0 < s < s_I$ and $F''(s) < 0$ for $s_I < s < 1$. When $s_A < s_I < s_B$, or $s_B < s_I < s_A$, the disturbance takes the form of a front followed by an expansion wave. At the passage of the front s changes discontinuously from its value s_A to a value $s_f > s_I$ given by

$$F'(s_f) = \frac{F(s_f) - F(s_A)}{s_f - s_A}. \tag{11.16}$$

In the centered wave $s_f < s < s_B$, or $s_B < s < s_f$; at its head the front is given by $r/R = \sqrt{F'(s_f)}$ and at its tail $r/R = \sqrt{F'(s_B)}$. The flows described in this paper are examples of this case with $s_A = 0$ and $s_B = 1$. When $s_I < s_A < s_B$, or $s_B < s_A < s_I$, the centered wave is not preceded by a front across which s is discontinuous. At its head $r/R = \sqrt{F'(s_A)}$ and at its tail $r/R = \sqrt{F'(s_B)}$. When $s_A < s_B < s_I$, or $s_I < s_B < s_A$, the flow consists of a front, at which

$$r/R = \sqrt{\frac{F(s_B) - F(s_A)}{s_B - s_A}}, \tag{11.17}$$

separating the region ahead where $s = s_A$ from the region behind where $s = s_B$: there is no centered wave.

The radially symmetric flow pattern is determined once the s_i have been specified ahead and behind the disturbance. Figure 9 depicts one of the *many* possible patterns for a three phase fluid. Ahead of the disturbance $\mathbf{s} = (s_1, s_2) =$ constant, $= \mathbf{s}_A$. The head of the disturbance is a front followed by a first expansion fan, followed by a region in which $s =$ constant, $= \mathbf{s}_M$, followed by a second front then by a second expansion fan, and finally by a second region in which $s =$ constant, $= \mathbf{s}_B$. $\mathbf{s}_A$ and $\mathbf{s}_B$ are specified, but $\mathbf{s}_M$ is unknown

https://doi.org/10.1017/S0956792500004289 Published online by Cambridge University Press

and must be determined. Let $(1/Q_1^2(s), 1/Q_2^2(s))$ be the two distinct eigenvalues, and $(\mathbf{r}_1(\mathbf{s}), \mathbf{r}_2(\mathbf{s}))$ corresponding right eigenvectors, of the 2×2 matrix $(\partial F_i/\partial s_j)$, $(i, j) = 1, 2$. Then, with $Q_2(\mathbf{s}_B) > Q_1(\mathbf{s}_B)$, in the expansion fans shown in Figure 9

$$\frac{d\mathbf{s}}{dQ} = \frac{\mathbf{r}_i}{\mathbf{r}_i \cdot \nabla_{\mathbf{s}} Q_i}, \; i = 1, 2. \tag{11.18}$$

In the first expansion fan equations (11.18) must be solved for $\mathbf{s} = \mathbf{s}_1(Q)$ subject to the conditions that when $Q = Q_1(\mathbf{s}_{f1})$

$$\mathbf{s}_1 = \mathbf{s}_{f1} \tag{11.19}$$

where, with $\mathbf{F}(\mathbf{s}) = (F_1(\mathbf{s}), F_2(\mathbf{s}))$, $\mathbf{s}_{f1}$ is determined from the front conditions

$$\mathbf{s}_{f1} - \mathbf{s}_A = Q_1^2(\mathbf{s}_{f1})(\mathbf{F}(\mathbf{s}_{f1}) - \mathbf{F}(\mathbf{s}_A)). \tag{11.20}$$

In the second expansion fan equations (11.18) must be solved for $\mathbf{s} = \mathbf{s}_2(Q)$ subject to the conditions that

$$\text{when } Q = Q_2(\mathbf{s}_B), \; \mathbf{s}_2 = \mathbf{s}_B. \tag{11.21}$$

It remains to determine Q which is equal to Q_{b1} at the back of the first fan and to Q_{f2} at the second front. Then, if $\mathbf{s}_{f2}$ denotes the value of $\mathbf{s}$ behind the second front,

$$\mathbf{s}_M = \mathbf{s}_1(Q_{b1}) \text{ and } \mathbf{s}_{f2} = \mathbf{s}_2(Q_{f2}). \tag{11.22}$$

With $\mathbf{s}_M$ and $\mathbf{s}_{f2}$ given by (11.22), Q_{b1} and Q_{f2} are determined from the front conditions

$$\mathbf{s}_{f2} - \mathbf{s}_M = Q_2^2(\mathbf{s}_{f2})(\mathbf{F}(\mathbf{s}_{f2}) - \mathbf{F}(\mathbf{s}_M)). \tag{11.23}$$

The procedure described above, which in practice must be a numerical procedure, determines the range of Q together with

$$\mathbf{s} = \mathbf{S}(Q) \text{ and } \lambda = \Lambda(Q) \tag{11.24}$$

in all regions of the flow domain. All other possible flow patterns can be obtained as obvious limiting cases. The procedure can be generalized to multi-phase fluids.

According to (11.13), when conditions (11.24) hold *all* equations (11.8) are satisfied if $Q(x, y, R)$ satisfies the single equation

$$Q^2 \frac{\partial Q}{\partial R} + u \frac{\partial Q}{\partial x} + v \frac{\partial Q}{\partial y} = 0. \tag{11.25}$$

With $u = Q \cos\beta$, $v = Q \sin\beta$ and $\lambda = \Lambda(Q)$, *equations* (11.5) and (11.25) *for* Q, β *and* p *are identical to those governing self-similar flows of two phase fluids.* Accordingly, the representations obtained for two-phase fluids can be used to describe self-similar flows of multi-phase fluids that are not radially symmetric. The representations yield an exact description of the flow only in some neighbourhood of the head of the disturbance. However, by the time all of the fronts are almost circular they do provide a good first approximation to the flow well behind the head of the disturbance.

12 Darcy and Hele-Shaw cell flows

With slight modifications, the analysis described above may be used to describe two other types of self-similar flows that are related to flows in porous media. First are Darcy flows

https://doi.org/10.1017/S0956792500004289 Published online by Cambridge University Press

of a single phase fluid that are generated by injecting the fluid into a region that initially contains no fluid. Second are Hele-Shaw cell flows in which one viscous fluid is driven by injecting some other viscous fluid; the fluids are immiscible and are either Newtonian or non-Newtonian. For both types of flow the front, or interface, is a material surface across which the pressure is continuous. The rate of flow across any closed curve surrounding the region where the fluid is injected is $2\pi r_0^2 R(t)R'(t)$.

12.1 Darcy flows

With the variables normalized as in § 5, the flow behind the front is governed by equations (5.1) and (5.2) with $\lambda =$ constant. At the front $R = W(x, y)$,

$$p = 0 \quad \text{and} \quad \cos\beta \frac{\partial W}{\partial x} + \sin\beta \frac{\partial W}{\partial y} = Q_f^{-1}. \tag{12.1}$$

For self-similar flows the expressions (7.14) and (7.16) for ψ and p reduce to

$$\psi = \beta R + \Psi - Q\frac{\partial \Psi}{\partial Q} \tag{12.2}$$

and

$$p = \log(Q/Qf)R + P - \frac{\partial \Psi}{\partial \beta}. \tag{12.3}$$

$x(R, \beta, Q)$ and $y(R, \beta, Q)$ are given by (8.4) and (8.5). $\Psi(\beta, Q)$ and $P(\beta, Q)$ satisfy equations (6.9) and (8.7) with $G = Q/\lambda$. The condition that $p = 0$ when $Q = Q_f$, together with equations (6.9) and (12.3), imply that $A(\beta)$ and $B(\beta)$ defined by (7.3) are related by (7.9). Finally, comparing equations (7.2) and (12.1) yields the result that $Q_f = 1$. It follows that with $Q_f = 1$ and $\lambda_o(0) = \lambda$, the flow is described by relations (9.10)–(9.12).

The representations (9.11) and (9.12) for $z(\zeta, R)$ and $\Phi(\zeta, R)$ are valid only when the image of the material surface at which $p = 0$ is the unit circle $|\zeta| = 1$ in the $\zeta-$plane. The general problem of determining flows in the vicinity of a material surface at which $p = 0$ reduces to that of finding $z(\zeta, R)$ and $\Phi(\zeta, R)$, which are analytic functions of ζ, satisfying the equation

$$\frac{\partial \Phi}{\partial \zeta} = \zeta^{-1}\frac{\partial z}{\partial \zeta} \tag{12.4}$$

and the *free boundary* condition that

$$\text{when } \mathrm{Re}(\Phi) = 0, \ \mathrm{Re}\left(\overline{\zeta}\left(\frac{\partial z}{\partial R} - \zeta\frac{\partial \Phi}{\partial R}\right)\right) = 1. \tag{12.5}$$

This last condition follows from the fact that at any material particle

$$\frac{dz}{dR} = u + iv = Qe^{i\beta} = \overline{\zeta}^{-1} \tag{12.6}$$

or

$$\overline{\zeta}\left(\frac{\partial z}{\partial R} + \frac{d\zeta}{dR}\frac{\partial z}{\partial \zeta}\right) = 1. \tag{12.7}$$

https://doi.org/10.1017/S0956792500004289 Published online by Cambridge University Press

Since

$$\frac{d\Phi}{dR} = \frac{\partial \Phi}{\partial R} + \frac{d\zeta}{dR}\frac{\partial \Phi}{\partial \zeta}, \tag{12.8}$$

it follows that

$$\overline{\zeta}\left(\frac{\partial z}{\partial R} - \zeta\frac{\partial \Phi}{\partial R}\right) + \zeta\overline{\zeta}\frac{d\Phi}{dR} = 1. \tag{12.9}$$

In particular, at any particle where $p = 0$ and $\Phi = i\psi$

$$\overline{\zeta}\left(\frac{\partial z}{\partial R} - \zeta\frac{\partial \Phi}{\partial R}\right) + i\zeta\overline{\zeta}\frac{d\psi}{dR} = 1 \tag{12.10}$$

and so conditions (12.5) hold. When z and Φ are given by (9.11) and (9.12) these conditions hold when $|\zeta| = 1$. Other solutions, describing flows that are not self-similar, are obtained by writing

$$\Phi = R\log\zeta + \sum_{n=-\infty}^{n=\infty}(n+1)\Phi_n(R)\zeta^n \quad \text{and} \quad z = \zeta\left(R + \sum_{n=-\infty}^{n=\infty} n\Phi_n(R)\zeta^n\right). \tag{12.11}$$

For example, if

$$\zeta_f = \sqrt{1 \pm (R_f/R)^2}\,, \tag{12.12}$$

where R_f is a constant, the relations

$$z = R\zeta + \frac{1}{2}\sum_{n=2}((n+1)C_n(\zeta/\zeta_f)^{(1-n)} - (n-1)\overline{C}_n(\zeta/\zeta_f)^{(n+1)}) \tag{12.13}$$

$$\Phi = -\lambda p + i\psi = R\log(\zeta/\zeta_f) + \frac{1}{2\zeta_f}\sum_{n=2} n^{-1}(n^2-1)(C_n(\zeta/\zeta_f)^{-n} - \overline{C}_n(\zeta/\zeta_f)^n) \tag{12.14}$$

describe *all* possible flows for which the normal velocity of the front depends only on time and does not vary with position on the front. The complex potential for the most general radially symmetric flow,

$$\Phi = R\log\left(\frac{z}{\sqrt{R^2 \pm R_f^2}}\right), \tag{12.15}$$

is obtained by taking the $C_n = 0$. When fluid is injected $R'(t) > 0$ and the plus sign must be taken in (12.12). Then (12.13) and (12.14) describe flows that are not self-similar for all $R(t)$, but which asymptote to the self-similar flows described by (9.10)–(9.12) as $R_f/R \to 0$. When fluid is extracted $R'(t) < 0$ and the minus sign must be taken in (12.12). In both cases, at the front $|\zeta| = \zeta_f$ and its speed, which equals the speed of the fluid, is $r_0R(t)R'(t)/\sqrt{R^2(t) \pm R_f^2}$.

As examples of flows in which the velocity of the front varies in both time and position consider the case when

$$z = R\zeta_0 Z(\eta) \quad \text{and} \quad \Phi = R\chi(\eta) \quad \text{where } \eta = \zeta/\zeta_0. \tag{12.16}$$

https://doi.org/10.1017/S0956792500004289 Published online by Cambridge University Press

Then, by (12.4) and (12.5),

$$Z'(\eta) = \eta\chi'(\eta) \tag{12.17}$$

and when

$$\mathrm{Re}(\chi) = 0, \mathrm{Re}(\overline{\eta}Z(\eta)) = 1. \tag{12.18}$$

These conditions can be satisfied by taking

$$Z = \sum_{n=-N}^{n=N} Z_n e^{n\chi}, \eta = \sum_{n=-N}^{n=N} nZ_n e^{n\chi}. \tag{12.19}$$

The $2N$ complex constants Z_n, $n = -N \cdots N$, satisfy the $(2N-1)$ nonlinear algebraic conditions

$$\sum_{n=-N}^{n=N} n|Z_n|^2 = 1 \quad \text{and} \quad \mathrm{Re}\left(\sum_{n=-N}^{n=N} (n-k)\overline{Z}_n Z_{n-k}\right) = 0 \tag{12.20}$$

for all $-N \leqslant k \leqslant N$ except $k = 0$. The solutions given by (12.16)–(12.20) are special cases of those obtained by Howison, Ockendon & Lacey (1985), Howison (1986) and Entov & Etingof (1997). These were derived using techniques developed by Richardson (1972, 1981). When $N = 1$, without loss in generality,

$$z = \sqrt{\frac{R^2 \pm R_f^2}{1-m^2}}(e^{\Phi/R} + me^{-\Phi/R}), \tag{12.21}$$

where m is a constant with $0 \leqslant m \leqslant 1$. According to (12.21) the front, and all other isobars, are ellipses. The representation (12.21) was obtained first by Howison (1986) in his investigation of bubble growth in a Hele-Shaw cell.

12.2 Hele-Shaw cell flows

If h denotes the width of the cell and $(u(x,y,t), v(x,y,t))$ denote the components of the average fluid velocity, the lubrication flow equations are

$$u = q\cos\beta = -\lambda(q)\frac{\partial p}{\partial x} = \frac{\partial \psi}{\partial y}, \tag{12.22}$$

$$v = q\sin\beta = -\lambda(q)\frac{\partial p}{\partial y} = -\frac{\partial \psi}{\partial x}. \tag{12.23}$$

At the interface $t = w(x,y)$ separating the fluids

$$q\left(\cos\beta\frac{\partial w}{\partial x} + \sin\beta\frac{\partial w}{\partial y}\right) = 1. \tag{12.24}$$

This condition, together with the fact that the pressure is continuous at the interface, implies

$$[q\cos(\theta-\beta)] = 0 \quad \text{and} \quad [(q/\lambda)\sin(\theta-\beta)] = 0. \tag{12.25}$$

https://doi.org/10.1017/S0956792500004289 Published online by Cambridge University Press

When μ, the coefficient of viscosity, is a function of τ, the magnitude of the shear stress on planes parallel to the walls of the cell, $\lambda(q)$ is determined from the parametric relations

$$\lambda = \frac{h^2}{4(\tau_w)^3}\int_0^{\tau_w}\frac{\tau^2}{\mu(\tau)}d\tau, \quad q = \frac{h}{2(\tau_w)^2}\int_0^{\tau_w}\frac{\tau^2}{\mu(\tau)}d\tau. \tag{12.26}$$

The variable parameter τ_w represents the magnitude of the shear stress at the walls of the cell. For a power law fluid

$$\mu = \mu_0(\tau/\tau_0)^{\sigma} \text{ and } \lambda/\lambda_0 = (1-\sigma/3)^{\frac{1}{\sigma-1}}(q/q_0)^{\frac{\sigma}{\sigma-1}}. \tag{12.27}$$

where

$$\lambda_0 = \frac{h^2}{12\mu_0} \text{ and } q_0 = \frac{h\tau_0}{6\mu_0}. \tag{12.28}$$

In particular, for a Newtonian fluid ($\sigma = 0$) $\lambda = \lambda_0$.

Shear thinning fluids like visco-plastic (Bingham) fluids, and shear thickening fluids like dilatant (colloidal) fluids, are often modeled in simple shear by piecewise linear relations between τ and γ, the magnitude of the velocity gradient. When $\tau < \tau_0$, $\tau = \mu_0\gamma$; when $\tau > \tau_0$

$$\tau = \tau_0 + \mu_\infty(\gamma - \tau_0/\mu_0) = \mu_\infty\left(\frac{\tau}{\tau-(1-\mu_\infty/\mu_0)\tau_0}\right)\gamma. \tag{12.29}$$

Consequently, when

$$\tau < \tau_0,\ \mu = \mu_0 \text{ and when } \tau > \tau_0,\ \mu = \mu_\infty\left(\frac{\tau}{\tau-(1-\mu_\infty/\mu_0)\tau_0}\right). \tag{12.30}$$

It follows from (12.26) and (12.30) that when $q < q_0$, $\lambda = \lambda_0$ and when $q > q_0$

$$\lambda = \lambda_0\frac{(1-\overline{\mu})(1-3\overline{\tau}^2)+2\overline{\tau}^3}{2\overline{\mu}\overline{\tau}^3} \text{ and } q = q_0\frac{(1-\overline{\mu})(1-3\overline{\tau}^2)+2\overline{\tau}^3}{2\overline{\mu}\overline{\tau}^2}, \tag{12.31}$$

where the variable $\overline{\tau} = \tau_w/\tau_0$ varies in the range $[1,\infty]$ and the constant $\overline{\mu} = \mu_\infty/\mu_0$. Figure 10 shows λ versus q curves for typical values of $\overline{\mu}$; the scaling constants

$$\lambda_\infty = \frac{h^2}{12\mu_\infty} \text{ and } q_\infty = \frac{h\tau_0}{6\mu_\infty}. \tag{12.32}$$

For shear thinning fluids ($\overline{\mu} < 1$) $\lambda'(q) > 0$ and $\lambda_0 \leqslant \lambda \leqslant \lambda_\infty$; for shear thickening fluids ($\overline{\mu} > 1$) $\lambda'(q) < 0$ and $\lambda_\infty \leqslant \lambda \leqslant \lambda_0$.

For radially symmetric flows

$$q = R(t)R'(t)/r, \quad p = R(t)R'(t)\int_{q_f}^{q}\frac{dq}{q\lambda(q)}, \tag{12.33}$$

where

$$q_f = R'(t)(1 \pm R_f^2/R^2(t))^{-1/2}. \tag{12.34}$$

In the limit as $R_f/R \to 0$, the flow is self-similar and $q_f \to R'(t)$.

https://doi.org/10.1017/S0956792500004289 Published online by Cambridge University Press

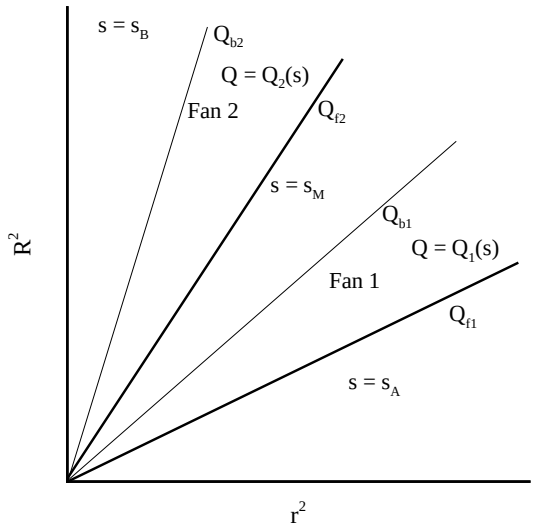

FIGURE 9. Example of a flow pattern in the radially symmetric flow of a three phase fluid.

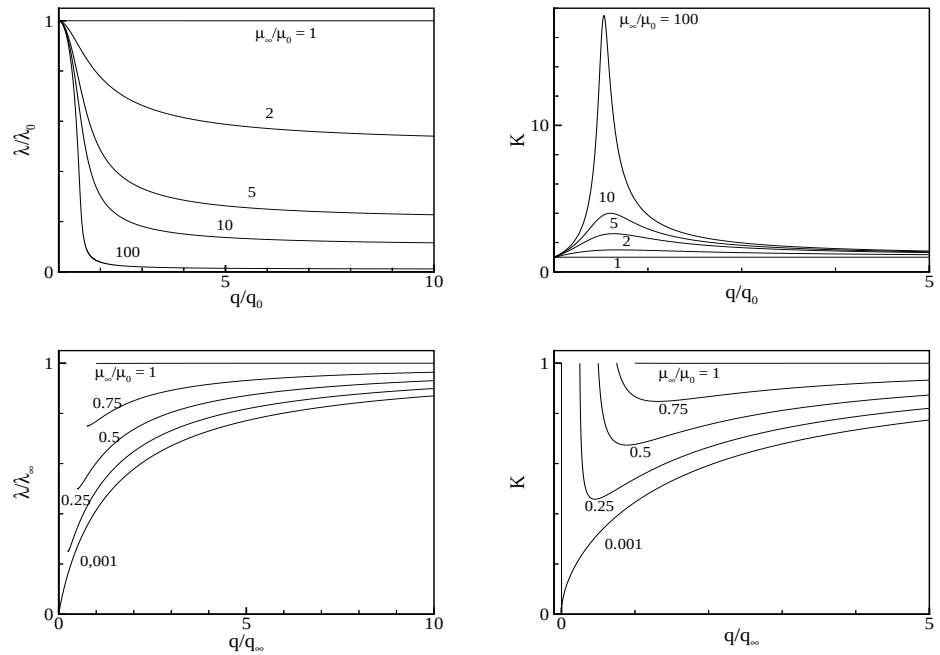

FIGURE 10. $\lambda(q)$ and $K(q)$ when the relation between shear stress and the rate of deformation is piecewise linear.

https://doi.org/10.1017/S0956792500004289 Published online by Cambridge University Press

12.3 Hodograph variables

If (β, q, t) are used as independent variables, the nonlinear equations (12.22) and (12.23) can *always* be replaced by an equivalent set of linear equations. Let ψ and p be expressed in terms of $\widehat{\psi}(\beta, q, t)$ and $\widehat{p}(\beta, q, t)$ as

$$\psi = \widehat{\psi} - q\frac{\partial \widehat{\psi}}{\partial q} \quad \text{and} \quad p = \widehat{p} - \frac{q}{K(q)}\frac{\partial \widehat{p}}{\partial q}, \tag{12.35}$$

where

$$K(q) = 1 - \frac{q\lambda'(q)}{\lambda(q)}. \tag{12.36}$$

Then $\widehat{\psi}$ and $\widehat{p}$ satisfy the equations

$$\frac{q}{\lambda(q)}\frac{\partial \widehat{\psi}}{\partial q} = -\frac{\partial \widehat{p}}{\partial \beta} \quad \text{and} \quad \left(\frac{q}{\lambda(q)}\right)'\frac{\partial \widehat{\psi}}{\partial \beta} = q\frac{\partial \widehat{p}}{\partial q}, \tag{12.37}$$

so that

$$q^2\frac{\partial^2 \widehat{\psi}}{\partial q^2} + K(q)\left(q\frac{\partial \widehat{\psi}}{\partial q} + \frac{\partial^2 \widehat{\psi}}{\partial \beta^2}\right) = 0. \tag{12.38}$$

In terms of $\widehat{\psi}(\beta, q, t)$,

$$x = \frac{\partial \widehat{\psi}}{\partial q}\sin\beta + q^{-1}\frac{\partial \widehat{\psi}}{\partial \beta}\cos\beta \quad \text{and} \quad y = -\frac{\partial \widehat{\psi}}{\partial q}\cos\beta + q^{-1}\frac{\partial \widehat{\psi}}{\partial \beta}\sin\beta, \tag{12.39}$$

or, more concisely,

$$z = q^{-1}e^{i\beta}\left(\frac{\partial \widehat{\psi}}{\partial \beta} - iq\frac{\partial \widehat{\psi}}{\partial q}\right). \tag{12.40}$$

For self-similar flows q is continuous, $= R'(t) = q_f(t)$, at the material interface separating the fluids and $\lambda(q)$ is discontinuous. It then follows from (12.25) that β is continuous, $= \theta$. For radially symmetric flows

$$\widehat{\psi} = R(t)R'(t)\beta, \ \widehat{p} = R(t)R'(t)\int_{q_f}^{q}\frac{K(q)}{q\lambda(q)}dq. \tag{12.41}$$

$$x = q^{-1}R(t)R'(t)\cos\beta, \quad \text{and} \quad y = q^{-1}R(t)R'(t)\sin\beta. \tag{12.42}$$

For flows that are not radially symmetric, write

$$\widehat{\psi} = R(t)R'(t)\beta + \widehat{\Psi}(\beta, q, t) \tag{12.43}$$

and

$$\widehat{p} = R(t)R'(t)\int_{q_f}^{q}\frac{K(q)}{q\lambda(q)}dq + \widehat{P}(\beta, q, t) \tag{12.44}$$

where $\widehat{\Psi}$ and $\widehat{P}$ satisfy the same equations as $\widehat{\psi}$ and $\widehat{p}$. In terms of $\widehat{\Psi}$

$$x = q^{-1}\left(R(t)R'(t) + \frac{\partial \widehat{\Psi}}{\partial \beta}\right)\cos\beta + \frac{\partial \widehat{\Psi}}{\partial q}\sin\beta \tag{12.45}$$

https://doi.org/10.1017/S0956792500004289 Published online by Cambridge University Press

$$y = q^{-1}\left(R(t)R'(t) + \frac{\partial \widehat{\Psi}}{\partial \beta}\right)\sin\beta - \frac{\partial \widehat{\Psi}}{\partial q}\cos\beta. \tag{12.46}$$

At the front

$$\text{when } q = q_f = R'(t), \quad \frac{\partial \widehat{\Psi}}{\partial \beta} = q_f A(\beta) \quad \text{and} \quad \frac{\partial \widehat{\Psi}}{\partial q} = -A'(\beta). \tag{12.47}$$

Also, the trajectory of the front is given by

$$x = (R(t) + A(\beta))\cos\beta - A'(\beta)\sin\beta \tag{12.48}$$

$$y = (R(t) + A(\beta))\sin\beta + A'(\beta)\cos\beta \tag{12.49}$$

$t = w(x, y)$ and $\beta = \beta(x, y)$ given by (12.48) and (12.49) satisfy equation (12.24) when $q = R'(t)$.

For power law fluids the problem for $\widehat{\Psi}(\beta, q, t)$ simplifies considerably. Since $\lambda \propto q^{\sigma/(\sigma-1)}$,

$$K(q) = (1-\sigma)^{-1}. \tag{12.50}$$

Then

$$\text{with } Q = q/q_f, \ \widehat{\Psi} = q_f \Psi(Q, \beta) \tag{12.51}$$

where

$$(1-\sigma)Q^2\frac{\partial^2 \Psi}{\partial Q^2} + Q\frac{\partial \Psi}{\partial Q} + \frac{\partial^2 \Psi}{\partial \beta^2} = 0. \tag{12.52}$$

The auxiliary conditions (12.47) require that, when

$$Q = 1, \quad \frac{\partial \Psi}{\partial \beta} = A(\beta) \quad \text{and} \quad \frac{\partial \Psi}{\partial Q} = -A'(\beta). \tag{12.53}$$

It follows that the representations (9.1)–(10.4) continue to hold with the $\Psi_\kappa(Q)$ satisfying the Euler equation

$$(1-\sigma)Q^2\Psi_\kappa'' + Q\Psi_\kappa' - \kappa^2\Psi_\kappa = 0 \tag{12.54}$$

with

$$\Psi_\kappa(1) = 1 \text{ and } \Psi_\kappa'(1) = \kappa^2. \tag{12.55}$$

When the fluid is non-Newtonian and is not a power law fluid K varies with q. (Figure 10 shows typical forms of $K(q)$ when the relation between τ and γ is piecewise linear.) If

$$A(\beta) = \sum_\kappa (A_\kappa \cos(\kappa\beta) + B_\kappa \sin(\kappa\beta)), \tag{12.56}$$

where summation is over some range of the parameter κ,

$$\widehat{\Psi} = \sum_\kappa \kappa^{-1}(A_\kappa \sin(\kappa\beta) - B_\kappa \cos(\kappa\beta))\widehat{\Psi}_\kappa(q, q_f) \tag{12.57}$$

where

$$q^2\frac{\partial^2 \widehat{\Psi}_\kappa}{\partial q^2} + K(q)\left(q\frac{\partial \widehat{\Psi}_\kappa}{\partial q} - \kappa^2\widehat{\Psi}_\kappa\right) = 0 \tag{12.58}$$

https://doi.org/10.1017/S0956792500004289 Published online by Cambridge University Press

with

$$\widehat{\Psi}_\kappa(q_f, q_f) = q_f \quad \text{and} \quad \frac{\partial \widehat{\Psi}_\kappa(q_f, q_f)}{\partial q} = \kappa^2. \tag{12.59}$$

It is easy to show that if $\Phi_\kappa(q)$ is *any* non-zero solution to the ordinary differential equation

$$q^2 \Phi_\kappa'' + K(q)(q\Phi_\kappa' - \kappa^2 \Phi_\kappa) = 0, \tag{12.60}$$

then

$$\widehat{\Psi}_\kappa(q, q_f) = q_f \frac{\Phi_\kappa(q)}{\Phi_\kappa(q_f)}(1 + h_\kappa(q_f) \int_{q_f}^{q} \frac{\lambda(q)}{q\Phi_\kappa^2(q)} dq) \tag{12.61}$$

where

$$h_\kappa(q_f) = \Phi_\kappa(q_f)(\kappa^2 \Phi_\kappa(q_f) - q_f \Phi_\kappa'(q_f))/\lambda(q_f). \tag{12.62}$$

One possible choice for $\Phi_\kappa(q)$ is $\widehat{\Psi}_\kappa(q, q_f(t_0))$, where t_0 denotes some reference time.

To summarize: with $\widehat{\Psi}$ given by relations (12.57)–(12.61), and with x and y given by (12.45) and (12.46),

$$\psi = R(t)R'(t)\beta + \sum_\kappa \kappa^{-1}(A_\kappa \sin(\kappa\beta) - B_\kappa \cos(\kappa\beta)) \left(\widehat{\Psi}_\kappa - q \frac{\partial \widehat{\Psi}_\kappa}{\partial q} \right) \tag{12.63}$$

and

$$p = R(t)R'(t) \int_{q_f}^{q} \frac{K(q)}{q\lambda(q)} dq + \frac{1}{\lambda(q)} \sum_\kappa \kappa^{-2} \, (A_\kappa \cos(\kappa\beta) + B_\kappa \sin(\kappa\beta)) \left(q \frac{\partial \widehat{\Psi}_\kappa}{\partial q} - \kappa^2 \widehat{\Psi}_\kappa \right). \tag{12.64}$$

Note that, according to (12.59) and (12.64), $p = 0$ at the interface separating the fluids. The representations given above are valid for any non-Newtonian fluids for which the shear modulus is a known function of the shear stress. The function $R(t)$ is arbitrary, and the shape of the front at any one time can be specified.

13 Conclusion

Hodograph techniques, that are usually used when the flow variables are functions of just two independent variables, are generalized to construct a class of exact solutions describing unsteady self-similar flows of multi-phase immiscible fluids. The techniques are used also to investigate the related problem of flows in a Hele-Shaw cell when the fluids involved are non-Newtonian. The flows are characterised by the fact that the sharp fronts, that separate the different phases or the different fluids, propagate with velocities that depend only on time. If the flows develop singularities in a finite time, capillary effects are locally important. When singularities are not produced, at large time the flows become radially symmetric.

https://doi.org/10.1017/S0956792500004289 Published online by Cambridge University Press

Acknowledgements

The research reported in this paper was supported in part by the Natural Sciences and Engineering Research Council of Canada under Grant A9117.

References

[1] Alexandrou, A. N. & Entov, V. M. (1997) On the steady-state advancement of fingers and bubbles in a Hele-Shaw cell filled by a non-Newtonian fluid. *Euro. J. Appl. Math.* **8**, 73–87.
[2] Barenblatt, G. I., Entov, V. M. & Ryzhik, V. M. (1990) *Flow of Fluids Through Natural Rocks.* Kluwer Academic.
[3] Chavent, G. & Jaffre, J. (1986) Mathematical models and finite elements for reservoir simulation. *Stud. in Math. & its Applic.* **17**, 1–51.
[4] Cumberbatch, E. & Varley, E. (1966) Generalized self-similar flows. *J. Inst. Math. Applic.* **2,** 1–11.
[5] Entov, V. M. & Etingof, P.I. (1996) Viscous flows with time-dependent free boundaries in a non-planar Hele-Shaw cell. *Euro. J. Appl. Math.* **8**, 23–35.
[6] Howison, S. D., Ockendon, J. R. & Lacey, A. A. (1985) Singularity development in moving-boundary problems. *Quart. J. Appl. Math.* **38,** 343–360.
[7] Howison, S. D. (1986) Bubble growth in porous media and Hele-Shaw cells. *Proc. Roy. Soc. Edin.* **102**, 141–148.
[8] Richardson, S. (1972) Hele-Shaw flows with a free boundary produced by the injection of fluid into a narrow channel. *J. Fluid Mech.* **4**, 609–618.
[9] Richardson, S. (1981) Some Hele-Shaw flows with time-dependent free boundaries. *J. Fluid Mech.* **102**, 263–278.
[10] Saffman, P. G. & Taylor, G, I. (1958) The penetration of a fluid into a porous medium or Hele-Shaw cell containing a more viscous liquid. *Proc. Roy. Soc. A*, **245**, 312–329.
[11] Sidorov, A. (1963) Generalized self-similar flows. *J. Appl. Math. Mech.* **27**, 1099–1108.
[12] Taylor, G. I. (1961) Interfaces between viscous fluids in narrow passages. *Problems of Continuum Mechanics,* SIAM, p. 546.
[13] Whitham, G. B. (1974) *Linear and Nonlinear Waves.* Wiley.
[14] EJAM (1995) Special issue, *Euro. J. Appl. Math.* **6**.
[15] EJAM (1999) Special issue, *Euro. J. Appl. Math.* **10**.